American Journal of Environmental Science and Engineering
2026, Vol. 10, No. 1, pp. 1–20
https://doi.org/10.11648/j.ajese.20261001.11

Research Article

Comparative Transcriptomics Reveals the Molecular Mechanism Underlying Heavy Metal Detoxification in Aspergillus Niger

Yingjie Chen, Yuyuan Duan, Tingfang Xue, Xinhui Deng*

School of Resource & Environment, Hunan University of Technology and Business, Changsha, China

Abstract

Aspergillus niger shows resistance to Zn and Cu; however, limited studies have evaluated the genetic mechanisms underlying metal tolerance in the species. In this study, comparative transcriptome analyses of *A. niger* F2 under Zn (4000 mg/L) and Cu (3000 mg/L) stress for 15 days were performed to identify genes involved in the response to heavy metal stress. There were more upregulated than downregulated genes under both Cu and Zn stress; however, more genes were differentially expre ssed under Cu than under Zn stress. Downregulated genes under Zn stress were enriched mainly in the membrane part of the cellular component category and for catalytic activity of ribonucleases in the molecular function category. Downregulated genes under Cu stress were enriched for import of Cu ions in the biological process category, intrinsic membrane in the cellula r component category, and reductase and oxidoreductase activity in the molecular function category. Differentially express ed genes under Zn and Cu stress were enriched for different functional domains based on Gene Ontology and Kyoto Ency clopedia of Genes and Genomes analyses. These findings indicated that under heavy metal stress, downregulated genes are mainly involved in ion transport and cell membrane-related functions. Furthermore, energy consumption was higher under Cu stress than under Zn stress, contributing to differences in tolerance levels for A. *niger*. These findings provide a b asis for genetic engineering for efficient bioremediation.

Keywords

Aspergillus, Differential Gene Expression, Heavy Metal Stress, Microbial Transcriptome

1. Introduction

The fungal genus *Aspergillus* is frequently used for the development of microbial cell factories owing to its diverse metabolites and specific mycelial structure. It is used to produce organic acids, proteins, and new bioactive secondary metabolites [1-3]. Species in the genus show strong resistance to heavy metals and are used as adsorbents and extracting agents for environmental control [4]. For example, *Aspergillus niger* has been used as an adsorbent for lead (Pb), cadmium (Cd), and copper (Cu) [5, 6] and for pigments [7]. The main biosorption mechanisms in A. *niger* are ion exchange, electronic attraction, and complexation (involving C=C, C-H, C-O, and N-H) [8, 9]. Metals are bioleached by A. *niger* from various substrates; the species has been used to bioleach valuable metals from spent catalysts, computer printed circuit boards, and

*Correspondence: Xinhui Deng (xhdeng2007@126.com)

Received: 30 December 2025; **Accepted:** 15 January 2026; **Published:** 11 February 2026

lithium-ion mobile phone batteries [10-12]. Scandium has been bioleached from bauxite residue while iron impurities have been bioleached from kaolin using A. *niger* [13, 14]. Additionally, heavy metals have been bioleached from contaminated soil using A. *niger* [15, 16]. The main bioleaching mechanisms for A. *niger* F2 include acidolysis, complexolysis (generation of organic acids), redoxolysis, and bioaccumulation [17].

Transcriptomics can improve our understanding of cell metabolism in polluted environments. In particular, transcriptome technology can rapidly predict relevant defense factors under stress and reveal relationships between metabolic pathways, signal transduction, and defense responses, providing a basis for improving microbial stress resistance and understanding the detoxification mechanisms under heavy metal stress [18]. In an early study, the structure and composition of the transcriptomes of two Prochlorococcus strains with a gene pool adapted to a specific environment were compared, revealing antisense transcription for 3/4 of all genes, hundreds of transcription start sites within genes with very little conservation, and non-coding transcripts differing between strains [19]. In Stenotrophomonas rhizophila, comparative transcriptomics analyses have revealed that pbt is responsible for adsorbing Pb^{2+}, phosphate permease is involved in the Pb^{2+} response, and czcA/cusA or Co^{2+}/Mg^{2+} efflux proteins contribute to the efflux of Pb^{2+} [20]. The impact of cadmium on Bacillus subtilis biofilms, morphology, and function was evaluated by transcriptomics. The main regulator of biofilm formation, Spo0A, decreased under Cd ion stress, inhibiting extracellular polysaccharide synthesis and the AbrB pathway. Cd ion treatment also increased the SigD content and expression levels of flagella-encoding and assembly genes in the strain [21].

Recent research on the transcriptome of *Aspergillus niger* has been aimed at improving enzyme production [22]. Wang et al. [23] developed a sucrose-inducible expression system based on the PfopA promoter and A. *niger* ATCC 20611. The system was successfully used to produce the monoenzyme β-glucosidase and a chitin-degrading enzyme cocktail including chitinase Chi46 and GlcNAcase NAG1 at high levels. The fermentation broths of recombinant strains can be directly applied to the substrate without additional purification, enabling efficient and cost-effective biomass degradation [23]. Additionally, studies have focused on characterizing transcriptional profiles under different conditions [24]. In A. *niger*, the transcriptional response to 6 h of exposure to wheat straw differed significantly from the response to 24 h of exposure to the same substrate, as determined using RNA sequencing [25]. In an analysis of spore germination, Novodvorska et al. [26] found that the transcriptome of dormant conidia was highly differentiated from that of germinating conidia, and major changes in response to an environmental shift occurred within the first hour of germination.

Detoxification mechanisms in microorganisms enable survival in environments polluted with heavy metals. These mechanisms include extracellular sequestration, redox transformation, efflux systems, methylation and volatilization, and biofilm collaborative defense. Extracellular sequestration is achieved by the adsorption or chelation of secreted extracellular polymers of heavy metals, cell surface adsorption, and mineral precipitation. Intracellular detoxification is achieved by chelating heavy metal ions with small proteins rich in sulfhydryl groups (-SH), such as metallothionein (MTs), glutathione, and phytochelin (PCs), to form non-toxic complexes and transporting heavy metals to specific cellular compartments (such as vacuoles) for isolation through metallochaperone proteins (e.g., yeast YCF1 transports the Cd-GSH complex to the vacuole). The REDOX pathway changes the valence state of heavy metal ions. Heavy metals with high toxicity are reduced to those with low toxicity or to easy precipitation valence states through REDOX enzymes (e.g., Hg^{2+} is reduced to Hg^{0}, Cr^{6+} to Cr^{3+}, and As^{5+} to As^{3+}). The main proteins involved in active efflux are ATPase pumps (P-type ATPases), CDF family proteins (ZnT), and RND family proteins. Bacterial CadA depends on ATP to discharge Cd^{2+}, Pb^{2+}, etc. ZnT transfers Zn^{2+} and Cd^{2+} to extracellular compartments or vacuoles, and the Cus system of Escherichia coli removes Cu+/Ag+. Methylation products, such as As methyltransferase in fungi, can translate As^{3+} into methylarsenic and some volatile products, such as dimethylselenium and dimethylmercury. Biofilm cooperative defense mechanisms include group protection and microenvironmental regulation. Microorganisms enhance the overall resistance via shared extracellular polymeric substances and lateral transfer of resistance genes to achieve population protection. Reductive environments in biofilms promote the precipitation of heavy metals (e.g., Fe^{3+} to Fe^{2+}) to achieve microenvironmental regulation. Research on the mechanisms underlying microbial detoxification of heavy metals can provide guidance for bioremediation, as resistant or genetically engineered bacteria have been used to treat contaminated soil/water, and for environmental monitoring through the design of biosensors using microbial heavy metal response genes, such as meroperons.

Heavy metals are bioaccumulative, non-degradable, and not environmentally durable, and their toxic effects occur at low concentrations, Zn and Cu are common heavy metals present in the polluted soil of mines. Although various mechanisms thro ugh which microbes counter heavy metal toxicity have been determined [27], little is known about the gene expression in A. niger under heavy metal stress from the perspective of transcriptomics. Thus, in this study, based on the strong tolerance of A. niger to Zn and Cu [15], a transcriptome approach was used to elucidate the molecular mechanisms contributing to the res ponses to Zn and Cu exposure in *A. niger*. This study serves to identify genes involved in heavy metal tolerance in fungal c ells and to provide a scientific basis for the construction of an engineered strain.

2. Materials and Methods

2.1. Culture Under Heavy Metal Stress and Transcriptome Sequencing

Liquid media were prepared as described by Deng et al. [9]. A spore suspension (1 mL) was cultured in 49 mL of liquid medium, the spores were harvested from the solid medium, and 15 samples were prepared and divided into three groups: 4000 mg/L Zn was added to group A, 3000 mg/L Cu was added to group B, and no heavy metal was added to group C. Each group consists of 3 repetitions. All samples were cultured for 15 days and then filtered. Mycelia were collected in a freezing tube, f rozen in liquid nitrogen for 30 min, preserved in a -80 ℃ refrigerator, and sent to Sangon Biotech (Shanghai) Co., Ltd. for tra nscriptomic sequencing (no reference genome). The mRNA library was constructed using the VAHTS™ mRNA-seq V2 Librar y Prep Kit for Illumina® (Nanjing Novizan), and the library was detected through 8% PAGE. The recycled DNA was accurate ly quantified using a Qubit2.0 DNA Detection Kit, made in Thermo Fisher Scientific, mixed at a ratio of 1:1, and sequenced.

2.2. Analysis of Transcriptome Sequencing Data

Illumina HiSeq™ raw image data files were analyzed using CASAVA Base Calling and converted to raw reads/raw data. Clean reads were obtained by removing reads with joints, with an N ratio of >5%, or with a mean quality <20. The quality control results are shown in Table 1. Overlapping reads were assembled into fragments using Trinity software (version 2.4.0) and further assembled into unigenes. Unigenes were also checked for redundancy and further spliced using Tgicl software (v2.0.6).

Table 1. *Quality control data for all samples.*

Item	A1	A2	A3	B1	B2	B3	C1	C2	C3
Total Read Count (bp)	53462316	56580574	58250714	60306476	50165442	62254234	59915350	37981956	45818770
Total Base Count (bp)	7799922526	8232441426	8539144295	8842535892	7338665769	9109868248	8757236715	55362377 77	6765581236
Average Read Length (bp)	145.9	145.5	146.59	146.63	146.29	146.33	146.16	145.76	147.66
Q10 Base Count (bp)	7799861752	8232377865	8539079954	8842468564	7338608593	9109793657	8757168882	55362202 13	6765527775
Q10 Base Ratio (%)	100.00%	100.00%	100.00%	100.00%	100.00%	100.00%	100.00%	100.00%	100.00%
Q20 Base Count (bp)	7753259917	8179973542	8484155171	8789274716	7292127824	9053973516	8704413955	54689303 25	6719240496
Q20 Base Ratio (%)	99.40%	99.36%	99.36%	99.40%	99.37%	99.39%	99.40%	98.78%	99.32%
Q30 Base Count (bp)	7594334688	8003589983	8297975402	8607326410	7135848373	8862789155	8522612759	52872151 47	6562816477
Q30 Base Ratio (%)	97.36%	97.22%	97.18%	97.34%	97.24%	97.29%	97.32%	95.50%	97.00%
N Base Count (bp)	60774	63561	64341	67328	57176	74591	67833	17564	53461
N Base Ratio (%)	0.00%	0.00%	0.00%	0.00%	0.00%	0.00%	0.00%	0.00%	0.00%
GC Base Count (bp)	4411946663	4618611250	4763806026	4963075619	4036200979	5080221015	4790932607	30397402 85	3699814435

Item	A1	A2	A3	B1	B2	B3	C1	C2	C3
GC Base Ratio (%)	56.56%	56.10%	55.79%	56.13%	55.00%	55.77%	54.71%	54.91%	54.69%

The transcripts were blast-searched using NCBI Blast+ against the following databases to acquire the functional annotation information: Eukaryotic Orthologous Groups (KOG), Swiss-Prot, TrEMBL, CDD, Gene Ontology (GO), and Kyoto Encyclopedia of Genes and Genomes (KEGG) (e-value < 0.00001). Annotation information was obtained from GO, SWISS- PROT, and TrEMBL. An automatic annotation server was used to obtain annotation information using KEGG. CDS prediction was carried out through comparisons using the BLAST database and TransDecoder. The valid data for the samples were compared with the transcripts obtained by splicing using Bowtie2, and mapping information was calculated. RSeQC was used to analyze redundant sequences and insert fragment distributions based on the comparison results. BEDTools was used to evaluate homogeneity and gene coverage. Salmon was used to calculate gene expression, represented by transcripts per million reads (TPM). The DESeq2 model was used to select differentially expressed genes ($q < 0.05$ and $|FoldChange| > 2$) [28]. For visualization, a scatter diagram was drawn based on the results of DEG screening. ClusterProfiler was used for KEGG pathway and KOG classification enrichment analyses. An association analysis network was drawn based on the results of the functional enrichment analysis.

2.3. Verification Through Quantitative Real-Time Polymerase Chain Reaction (qRT-PCR)

For verification, quantitative real-time polymerase chain reaction (qRT-PCR) was perfomed by the Wuhan Institute of Biotechnology. In particular, 28 genes were selected for verification using the BIO-RAD CFX Connect™ Fluorescence Quantitative PCR Detection System and Power SYBR® Green PCR Master Mix (Applied Biosystems® Cat: 4367659). The same RNA samples were used for Illumina library synthesis and qRT-PCR verification. The specific primers used for qRT-PCR are listed in Additional File 1, and actin and β-tubulin were used as endogenous controls. Relative gene expression was analyzed using the comparative threshold (CT) cycle method established by Livak & Schmittgen [29].

First, the CT value for the target gene was normalized to that of the reference gene (ref) for both test and calibrator samples as follows:

ΔCT (test) = CT (target, test) – CT (ref, test)

ΔCT (calibrator) = CT (target, calibrator) – CT (ref, calibrator)

Second, the ΔCT value for the test sample was normalized to the ΔCT value for the calibrator: $\Delta\Delta$CT =ΔCT (test) – ΔCT (calibrator)

Finally, the expression ratio was calculated as follows: $2^{-\Delta\Delta CT}$ = Normalized expression ratio

3. Results and Dicussion

3.1. Transcriptome Profiles and Splicing Under Zn and Cu Stress

After quality control, 183324 transcripts and 90345 unigenes were assembled. The maximum length of transcripts or unigenes was 16168 base pairs (bp), minimum length was 201 bp, and average transcript lengths were 1607.79 bp and 836.17 bp for unigenes (Table 2). The mapping ratios for all samples exceeded 97%, and the average ratios of multiply mapped samples were 81.61% for samples under Zn stress, 80.27% for samples under Cu stress, and 82.91% for control samples. The average ratios of uniquely mapped reads were 16.21% for samples under Zn stress, 17.35% for samples under Cu stress, and 14.70% for controls (Table 3). Regarding coverage, 8393, 9450, and 7573 genes showed values between 90% and 100% for samples under Zn stress, 20254, 11094, and 14889 genes were between 90% and 100% for samples under Cu stress, and 8575, 4788, and 14245 genes were between 90% and 100% for controls (Table 4). These findings indicated that transcriptome sequencing and splicing results for *A. niger* were accurate and reliable.

Table 2. *Assembly results.*

Item	No.	≥500 bp	≥1000 bp	N50	N90	Max Length (bp)	Min Length (bp)	Total Length (bp)	Average Length (bp)
Transcript	183324	108547	83291	3263	719	16168	201	294746548	1607.79

Item	No.	≥500 bp	≥1000 bp	N50	N90	Max Length (bp)	Min Length (bp)	Total Length (bp)	Average Length (bp)
Unigene	90345	32441	20933	1876	263	16168	201	75544213	836.17

Table 3. Mapping results for Aspergillus niger.

Item	A1 (%)	A2 (%)	A3 (%)	B1 (%)	B2 (%)	B3 (%)	C1 (%)	C2 (%)	C3 (%)
Total reads	100.00	100.00	100.00	100.00	100.00	100.00	100.00	100.00	100.00
Total mapped	97.71	97.85	97.88	97.92	97.12	97.82	97.56	98.04	97.22
Multiple mapped	81.00	81.72	82.10	79.89	81.17	79.74	83.55	83.58	81.60
Uniquely mapped	16.71	16.13	15.78	18.04	15.95	18.07	14.01	14.46	15.62
Read-1 mapped	8.36	8.07	7.89	9.02	7.98	9.04	7.01	7.23	7.81
Read-2 mapped	8.35	8.06	7.89	9.02	7.97	9.04	7.00	7.23	7.81
Reads map to '+'	8.35	8.07	7.92	9.02	8.00	9.03	7.03	7.25	7.85
Reads map to '-'	8.36	8.05	7.86	9.02	7.95	9.04	6.98	7.21	7.77
Non-splice reads	16.71	16.13	15.78	18.04	15.95	18.07	14.01	14.46	15.62
Splice reads	0.00	0.00	0.00	0.00	0.00	0.00	0.00	0.00	0.00
Reads mapped in proper pairs	15.41	14.85	14.71	16.79	14.74	16.71	12.96	13.55	14.51

Table 4. Coverage of genes.

Item	A1	A2	A3	B1	B2	B3	C1	C2	C3
0%−10%	59188	57630	60157	44930	50771	43478	66913	71249	57765
10%−20%	1750	1093	1519	1897	1033	1547	561	2164	653
20%−30%	2006	1737	2045	1969	1784	2185	1022	1542	978
30%−40%	2292	2202	2198	2072	2691	2863	1306	1372	1395
40%−50%	2662	2638	2581	2357	3771	3638	1831	1421	2032
50%−60%	3036	3051	3091	2923	4323	4537	2179	1506	2760
60%−70%	3447	3553	3454	3605	5139	5113	2344	1644	3347
70%−80%	3494	3859	3658	4290	4871	5539	2522	1926	3429
80%−90%	4077	5132	4069	6048	4868	6556	3092	273	3741
90%−100%	8393	9450	7573	20254	11094	14889	8575	4788	14245

Note: A represents samples under Zn stress, B represents samples under Cu stress, and C represents the control

3.2. Screening and Annotation of Significantly Differentially Expressed Genes Under Zn and Cu Stress

The percentages of annotated genes were 28.43% in KOG, 57.59% in GO, and 8.01% in KEGG (Figure 1). When compared with results for group C, 6121 genes and 7568 transcripts with significant differences were screened from group A, including 5941 and 7256 upregulated genes and transcripts and 180 and 312 downregulated genes and transcripts, respectively (Figure 2a). Additionally, levels of 7975 genes and 10011 transcripts differed significantly between groups C and B, among which 7907 genes and 9764 transcripts were upregulated and 68 genes and 247 transcripts were downregulated in group B (Figure 2b). In total, 1352 genes and 1408 transcripts differed significantly between groups A and B, among which 17 genes and 79 transcripts were upregulated and 1335 genes and 1329 transcripts were downregulated in group B (Figure 2c). Under Cu stress, the activated genes (FC ≥ 20) were mainly enriched for protein synthesis, REDOX reaction, and copper chaperone (Table 5), which might owing to that Cu toxicity arises from catalyzing the formation of ROS via Fenton-like reactions or substitution for Fe-S clusters [30]. The activated genes under Zn stress (FC ≥ 20) were mainly enriched for zinc ion transport and REDOX and those with FC ≤ --18 were mainly related to zinc ion transport (Table 6). Most differentially expressed genes were upregulat ed, and only a few were downregulated under Zn or Cu stress, indicating that A. *niger* actively responded to Zn and Cu stres s by increasing the expression of related genes to maintain normal functions and physiology The adsorption-tolerance synergy i the main resistance mechanism *niger* under heavy metal stress [31].

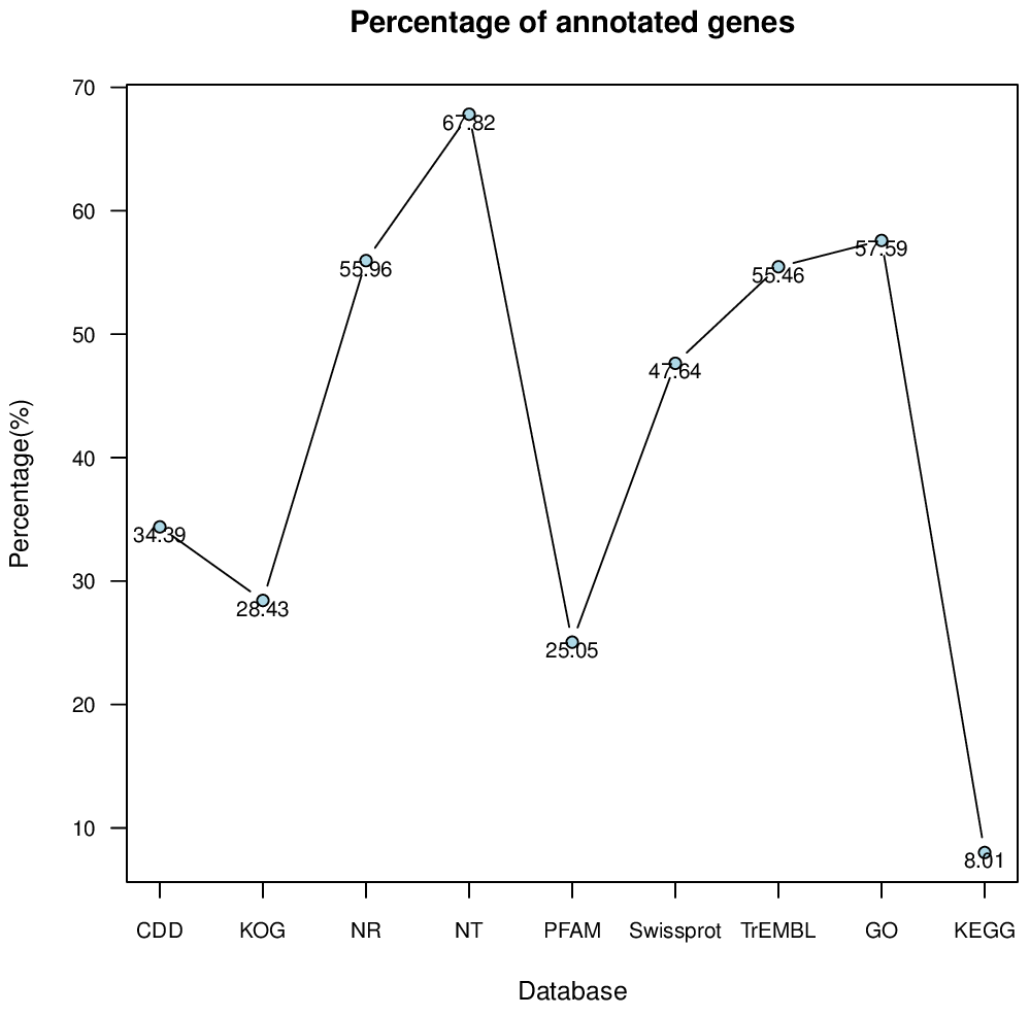

Figure 1. *Percentage of annotated genes in different database.*

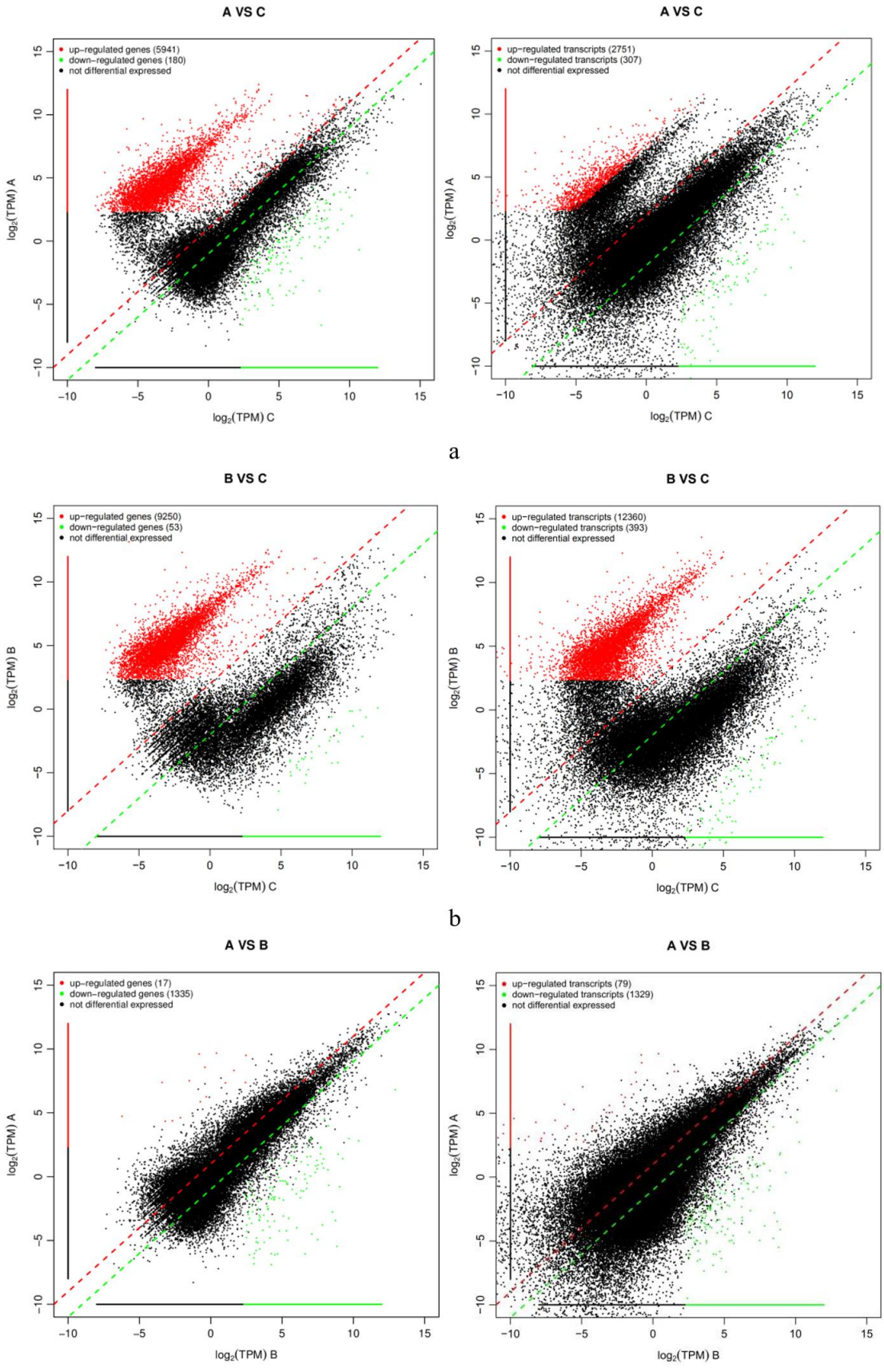

Figure 2. *The differential genes under Zn and Cu (qValue<0.05 and |FoldChange|>2).*

(a represents the different genes and transcripts of A vs C, b represents the different genes and transcripts of B vs C, c represents the different genes and transcripts of A vs B.)

Table 5. *Differential gene expression under Cu stress (FC ≥ 20 or ≤ -18).*

Gene id	Mean TPM (B)	Mean TPM (C)	log2 fold change	q-Value	Direction	Function (KOG/GO/TrEMBL)
TRINITY_DN37137 _c4_g3	1403.40 39	0.0001	23.74242701	3.54E- 07	up	Ubiquitin/60S ribosomal protein L40 fusion
TRIN-ITY_DN35856 _c0_g4	951.091 7	0.0001	23.18115305	4.12E- 08	up	Thioredoxin
TRIN-ITY_DN37465 _c0_g1	808.478 8	0.0001	22.94677842	4.82E- 14	up	Uncharacterized protein OS=*Aspergillus oryzae*
TRIN-ITY_DN37095 _c0_g2	550.070 3	0.0001	22.39118467	3.07E- 06	up	Ubiquitin/40S ribosomal protein S27a fusion
TRIN-ITY_DN36195 _c1_g9	484.202 3	0.0001	22.20717853	9.74E- 08	up	Copper chaperone
TRIN-ITY_DN35384 _c0_g2	369.312 2	0.0001	21.81640975	1.55E- 05	up	Molecular chaperones HSP70/HSC70, HSP70 super-family
TRIN-ITY_DN35885 _c2_g7	307.329 4	0.0001	21.55135425	5.65E- 06	up	Ubiquitin/60s ribosomal protein L40 fusion
TRIN-ITY_DN37185 _c0_g3	306.433 1	0.0001	21.54714087	1.28E- 07	up	NADH:flavin oxidoreductase/12-oxophytodienoate reductase
TRIN-ITY_DN35247 _c0_g4	294.128 3	0.0001	21.48801433	0.0005	up	Glutaredoxin and related proteins
TRIN-ITY_DN37215 _c0_g1	272.012 3	0.0001	21.37524034	2.79E- 07	up	/
TRIN-ITY_DN32067 _c0_g1	271.879	0.0001	21.37453329	0.0006	up	1-Acyl dihydroxyacetone phosphate reductase and related dehydrogenases
TRIN-ITY_DN36707 _c0_g1	235.113 7	0.0001	21.16492701	3.37E- 07	up	Molecular chaperones HSP70/HSC70, HSP70 super-family
TRIN-ITY_DN36887 _c2_g4	222.361	0.0001	21.08447234	3.16E- 06	up	Molecular chaperone (small heat-shock protein Hsp26/Hsp42)
TRIN-ITY_DN58047 _c0_g1	0.0001	37.9444	-18.53352746	0.0111	down	Subtilisin kexin isozyme-1/site 1 protease, subtilase superfamily
TRIN-ITY_DN35446 _c3_g1	0.0001	52.9275	-19.01365799	0.0115	down	Integral membrane component

Table 6. Differential gene expression under Zn stress (FC ≥ 20 or ≤ -18).

Gene id	Mean TPM (A)	Mean TPM (C)	log2 fold change	q-Value	Direction	Function
TRINITY_DN37048_ c0_g2	427.7188	0.0001	22.0282	2.60E- 09	up	Uncharacterized protein
TRIN-ITY_DN24487_ c0_g1	379.4474	0.0001	21.8556	2.60E- 09	up	/
TRIN-ITY_DN35247_ c0_g4	313.9668	0.0001	21.5822	2.72E- 06	up	/
TRIN-ITY_DN37802_ c1_g1	181.5296	0.0001	20.7918	8.50E- 09	up	Zn^{2+} transporter ZNT1 and related Cd^{2+}/Zn^{2+} transporters (cation dif-fusion facilitator superfamily)
TRIN-ITY_DN36989_ c0_g9	158.1992	0.0001	20.5933	3.26E- 08	up	oxidoreductase activity, acting on paired donors, with incorporation or reduction of molecular oxygen
TRIN-ITY_DN36642_ c0_g6	111.8162	0.0001	20.0927	3.08E- 08	up	oxidoreductase activity, acting on paired donors, with incorporation or reduction of molecular oxygen
TRIN-ITY_DN36908_ c0_g3	110.6152	0.0001	20.0771	1.65E- 07	up	/
TRIN-ITY_DN25819_ c0_g1	105.5342	0.0001	20.0093	2.36E- 08	up	oxidoreductase activity, acting on paired donors, with incorporation or reduction of molecular oxygen
TRIN-ITY_DN37305_ c0_g12	104.8678	0.0001	20.0001	2.36E- 07	up	zinc ion binding/oxidoreductase activity
TRIN-ITY_DN17316_ c0_g2	0.0001	27.6384	-18.0763	0.0353	down	cytoplasm/L-amino acid trans-membrane transporter activity
TRIN-ITY_DN37431_ c0_g3	0.0001	32.7865	-18.3227	0.0169	down	ribonuclease III activity/RNA binding/RNA processing
TRIN-ITY_DN22007_ c0_g1	0.0001	50.1727	-18.9365	9.06E- 05	down	integral membrane component
TRIN-ITY_DN35446_ c3_g1	0.0001	52.9275	-19.0137	0.0002	down	integral membrane component
TRIN-ITY_DN25218_ c0_g1	0.0001	122.6521	-20.2261	0.0002	down	/
TRIN-ITY_DN14417_ c0_g1	0.0001	192.1176	-20.8736	8.44E- 05	down	Unnamed protein product OS
TRIN-ITY_DN53309_ c0_g1	0.0001	861.5829	-23.03856	2.69E- 06	down	/

Table 7. Verified differentially expressed genes.

Gene id	Mean TPM (A)	Mean TPM (B)	Mean TPM (C)	log2 fold change	Q-Value	Result 1	Result 2
TRINITY_DN36226_c3_g1	911.3373	2.4437	/	8.5428	2.67E-06	up	up
TRINITY_DN37865_c1_g4	1602.097 9	5.7960	/	8.1107	6.89E-06	up	up
TRINITY_DN37487_c0_g1	2.6218	187.8221	/	-6.1627	0.0093	down	up
TRINITY_DN27566_c0_g1	1.8571	564.1446	/	-8.2469	0.0010	down	down
TRINITY_DN30178_c0_g1	23.8624	0.0001	/	17.8644	1.0000	up	up
TRINITY_DN37711_c1_g5	42.2521	0.0001	/	18.6887	2.13E-07	up	up
TRINITY_DN37502_c0_g5	43.4822	0.0001	/	18.7301	5.95E-05	up	up
TRINITY_DN35627_c0_g10	37.0141	0.0001	/	18.4977	1.05E-05	up	up
TRINITY_DN34499_c2_g1	16.9937	0.0001	/	17.3746	1.17E-06	up	up
TRINITY_DN35404_c2_g3	/	3222.3667	10.8374	8.2160	0.0006	up	down
TRINITY_DN37634_c1_g1	/	829.3407	4.3637	7.5703	0.0009	up	up
TRINITY_DN35878_c1_g1	/	6.2588	766.4338	-6.9361	0.0109	down	down
TRINITY_DN35561_c1_g1	/	6.3221	647.0381	-6.6773	0.0207	down	up
TRINITY_DN35178_c3_g1	/	91.5329	0.0001	19.8040	5.84E-06	up	up
TRINITY_DN37809_c0_g5	/	77.7409	0.0001	19.5683	2.93E-06	up	up
TRINITY_DN37260_c1_g3	/	53.6735	0.0001	19.0339	1.29E-06	up	up

Gene id	Mean TPM (A)	Mean TPM (B)	Mean TPM (C)	log2 fold change	Q-Value	Result 1	Result 2
TRINITY_DN36124_c2_g8	/	17.6184	0.0001	17.4267	0.0001	up	up
TRINITY_DN37249_c1_g12	/	29.7571	0.0001	18.1829	7.20E-06	up	up
TRINITY_DN37780_c0_g1	/	300.2814	7.8724	5.2534	0.0005	up	up
TRINITY_DN37780_c0_g1	15.8333	/	300.2814	-4.2453	0.0046	down	down
TRINITY_DN37749_c2_g8	5.7350	/	60.45897	-3.3981	0.0498	down	down
TRINITY_DN33158_c0_g1	2.3459	/	18.7670	-2.9999	0.0405	down	up
TRINITY_DN30925_c0_g1	2.0546	/	223.2975	-6.7640	0.0004	down	down
TRINITY_DN35913_c0_g2	315.0660	/	3.0729	6.6800	0.0264	up	down
TRINITY_DN37504_c2_g1	0.0001	/	241.8143	-21.2055	7.26E-07	down	down
TRINITY_DN21185_c0_g1	0.0001	/	95.4216	-19.8640	3.05E-06	down	down
TRINITY_DN35275_c1_g2	0.0001	/	117.9133	-20.1693	7.53E-06	down	down
TRINITY_DN36707_c0_g1	0.0001	/	235.1137	-21.1650	5.16E-07	down	down

Note: A represents samples under Zn stress, B represents samples under Cu stress, and C represents the controls.
Result 1 refers to the transcriptome sequencing results, while Result 2 refers to the qRT-PCR verification results. qRT-PCR, quantitative reverse transcription-polymerase chain reaction

3.3. Comparison of Differentially Expressed Genes Under Zn and Cu Stress

3.3.1. Characteristics of Gene Expression Under Zn Stress

Significantly differentially expressed genes were enriched for various terms in the GO database. Differentially expressed genes in A vs. C were mainly enriched in the following GO terms: cytoplasmic part, intracellular part, intracellular membrane-bound, intracellular organelle, cytoplasm, cell, intracellular, and cytosol (Figure 3a). Using KOG, there was significant enrichment for the terms RNA processing and modification, cell cycle control, cell division, chromosome partitioning, unknown function, replication, re-

combination and repair, amino acid transport, and metabolism (Figure 3b).

In A vs. C, no downregulated genes were significantly enriched in the biological processes category (q<0.001). It total, 54 significantly downregulated genes were enriched for the term membrane part in the cellular component category (q = 0.0042), indicating roles in integral and intrinsic components of the membrane (Figure 3c), including the regulation of the membrane channels of Zn ions and membrane proteins involved in Zn ion transport. Additionally, 74 significantly down-regulated genes were enriched for the term catalytic activity in the molecular function category (q = 0.5531), indicating a role in the regulation of double-stranded RNA-specific ribonuclease activity and ribonuclease III activity (Additional File 2). These findings imply that Zn induced damage in *A. niger* cell via two mechanisms: (1) the membrane structure of cells was affected to prevent Zn from entering cells and (2) ribonuclease activity was affected, preventing the hydrolysis of nucleic acids. The mechanism underlying resistance to Zn was observed at the molecular level. In the biological processes category, 3295, 2864, and 1239 upregulated genes were enriched for the terms cellular process (q = 0.0003), metabolic process (q = 0.0065), and cellular component organization or biogenesis (q = 0.0248), respectively. In the cellular component category, 3735, 3725, 1331, 3122, and 1957 upregulated genes were enriched for the terms cell, cell part, macromolecular complex, organelle, and organelle part (q = 0.0000), excluding nuclear replication fork, protein complex, mating projection, and mitochondrial ribosome, etc. In the molecular function category, 2544 upregulated genes were enriched for the term catalytic activity (q = 0.0016), indicating roles in processes related to RNA binding, nucleic acid binding, nuclease, ribonuclease, endonuclease, and endoribonuclease activity (Figure 3d). The upregulated genes were beneficial for DNA replication and protein synthesis.

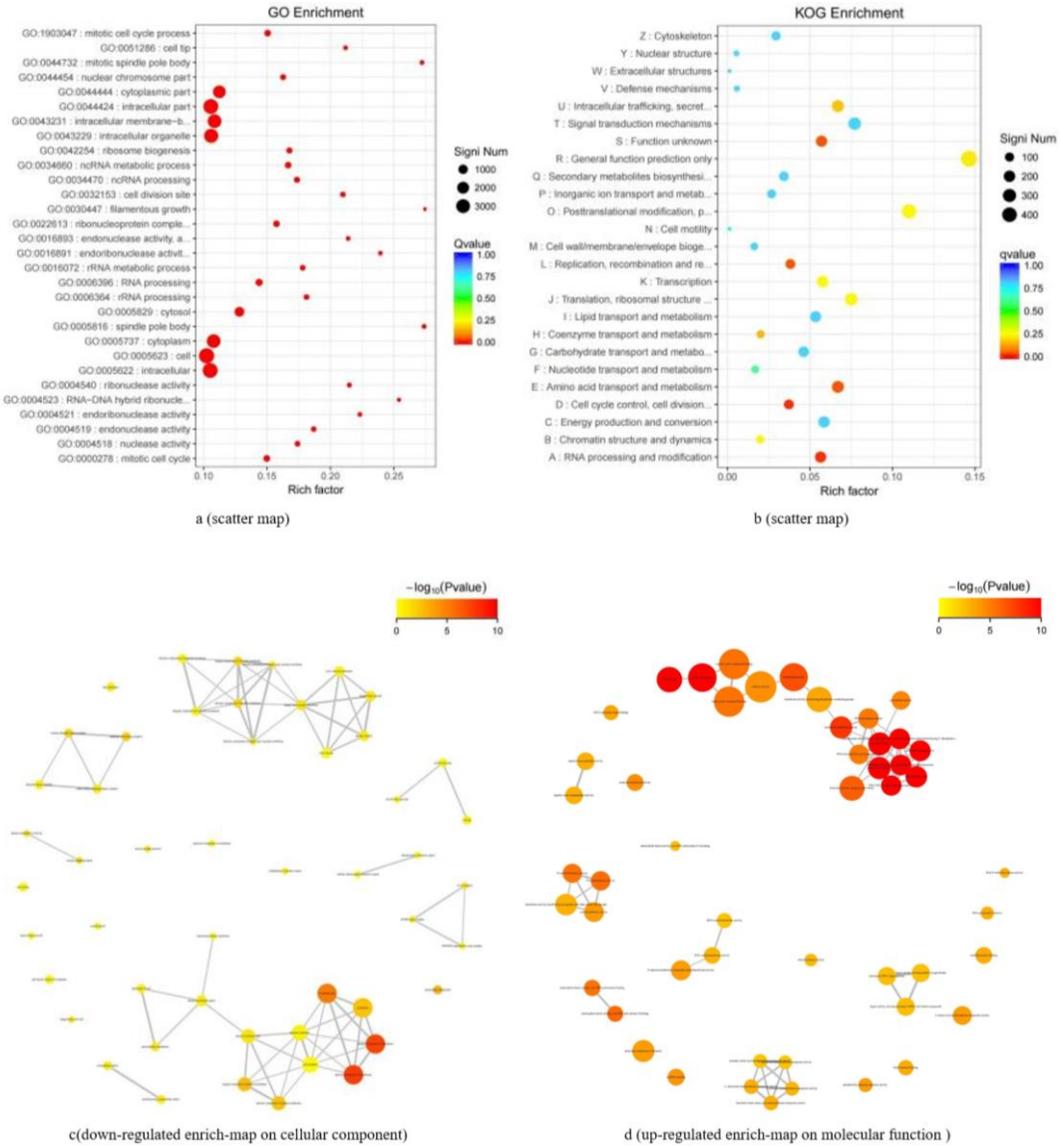

Figure 3. *The enrichment of the differential genes (Go database) (A vs C).*

In a KEGG enrichment analysis, the upregulated genes were mainly involved in three pathways, DNA replication, aminoacyl- tRNA biosynthesis, and ribosome biogenesis in eukaryotes (Figure 4a), concentrated in the category of genetic information processing and protein synthesis. Genes related to the metabolism of carbohydrates and energy were not upregulated. These findings confirmed that *A. niger* achieved resistance to Zn via the promotion of a wide range of biological processes, especially DNA replication and RNA and protein synthesis. The downregulated genes were significantly enriched in styrene, chloroalkane and chloroalkene, chlorocyclohexane and chloroalkene, dioxin, polycyclic aromatic hydrocarbon degradation, β- alanine, and tyrosine metabolism pathways (Figure 4b). The downregulated genes were involved in the metabolism of toxic substances, β-alanine, and tyrosine, indicating the reduced activity of enzymes involved in biochemical reactions under Zn stress. Tyrosine plays an important role in the protein surface and binding interface; the reduction in this metabolic pathway may cause a decline in membrane protein function. Additionally, β-alanine plays important roles in cell metabolism, energy, the maintenance of an acid-alkali balance, regulate protein synthesis, and other processes.

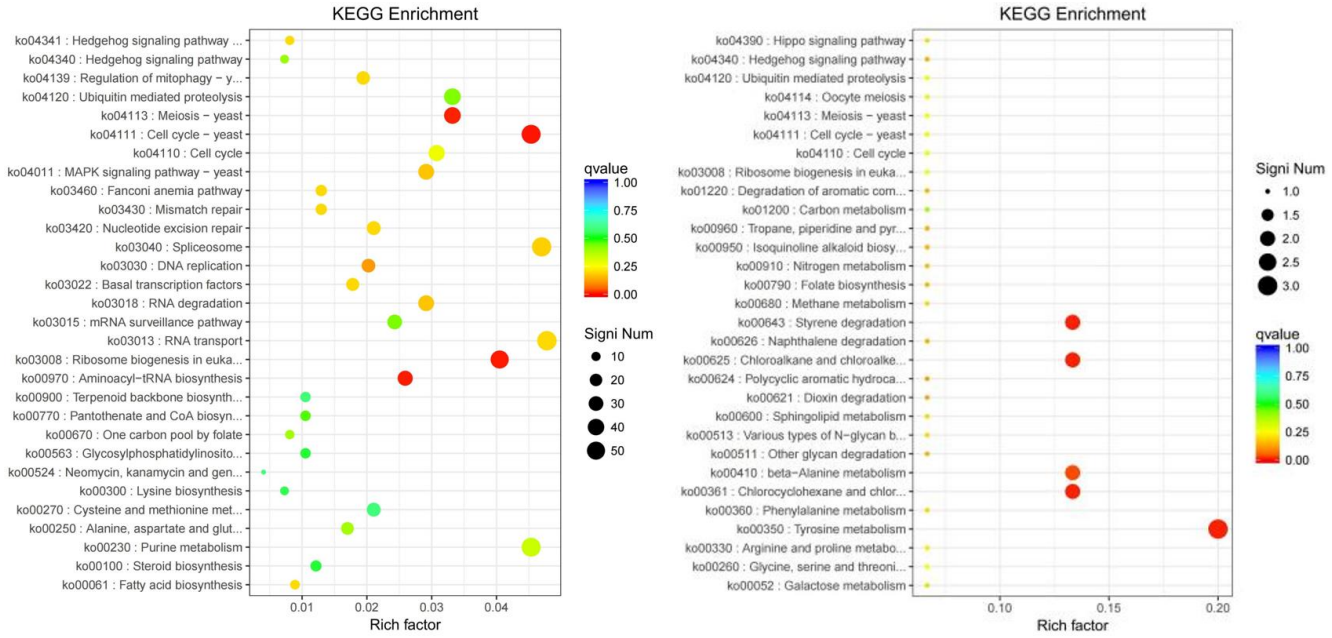

a (up-regulated differential genes) b (down-regulated differential genes)

Figure 4. *The enrichment of the differential genes (KEGG database)(A vs C).*

3.3.2. Characteristics of Gene Expression Under Cu Stress

Significantly differentially expressed genes between groups B and C were mainly enriched for the terms post-translational modification, protein turnover, chaperones; intracellular trafficking, secretion, and vesicular transport; energy production and conversion; and cell cycle control, cell division, chromosome partitioning according to the KOG mapping results (Figure 5a). Downregulated genes under Cu stress were enriched for the terms, ion transport, Cu ion transport and Cu ion import in the biological process category (Figure 5b), membrane part, intrinsic component of membrane, integral component of membrane in the cellular component category (Figure 5c), and ferric-chelate reductase and oxidoreductase activity in the molecular function category (Figure 5d). The downregulation of these genes suggests that *A. niger* maintains intracellular Cu ion homeostasis by changing the membrane structure and reducing the transport of Cu ions to limit input; excess Cu ions are bound to proteins during the tricarboxylic acid cycle, inducing the heteromerization of these proteins, resulting in reduced activity of iron-containing reductase [32]. Physiological processes, such as energy metabolism, organic degradation, and antioxidant defense, were affected by Cu-ion stress in *A. niger*.

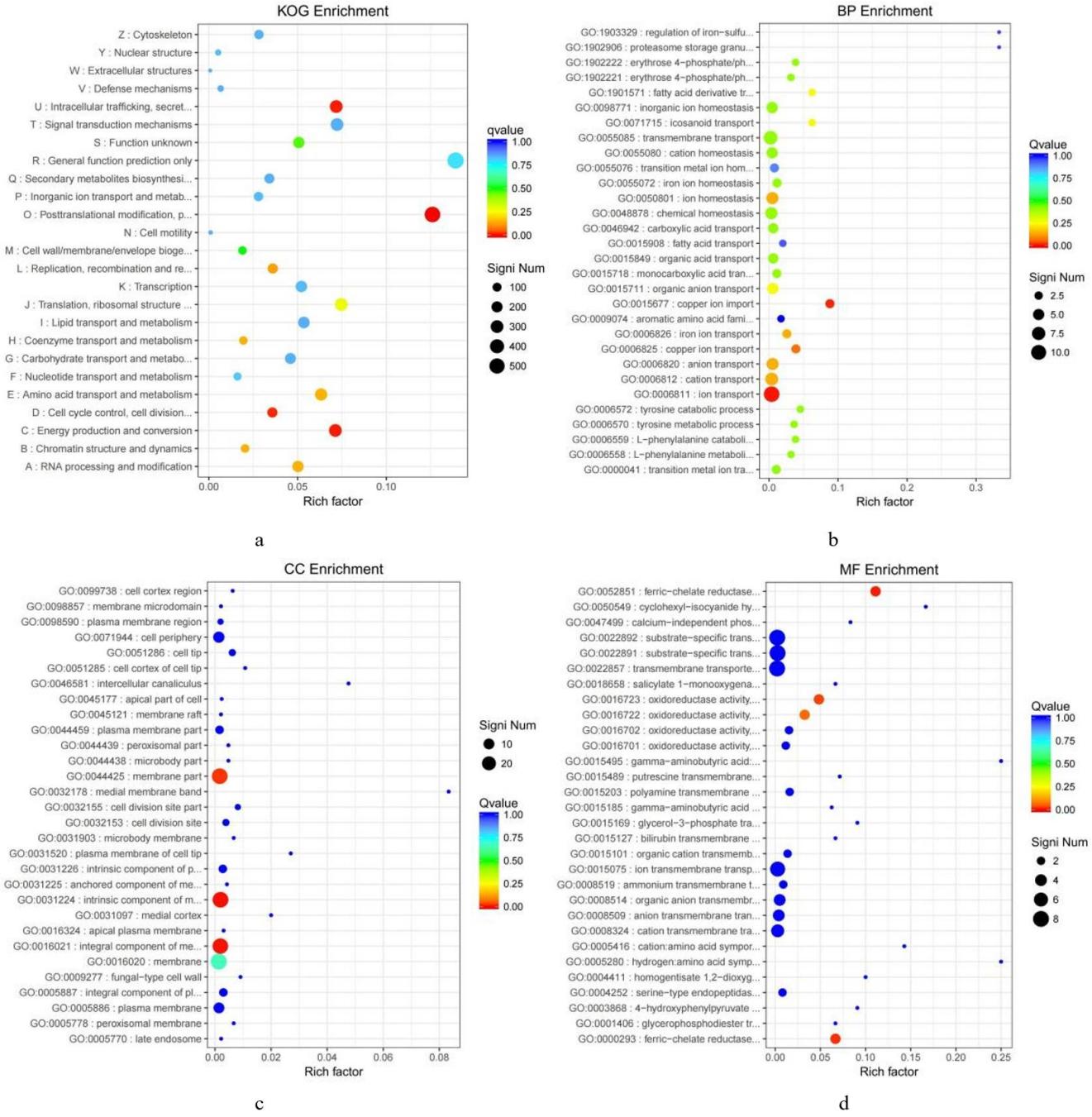

(a-the significantly differential genes in KOG; b,c,d- the down-regulated significantly differential genes in GO)

Figure 5. *The enrichment of the significantly differential genes (B vsC).*

Most of the significantly differentially expressed genes in *A. niger* were upregulated. In the biological process category, 4203 upregulated genes were associated with cellular processes (q = 0.0182) and 3665 upregulated genes were associated with metabolic processes (q = 0.0065). In the cellular component category, 4794 upregulated genes were associated with the term cell (q = 0.0000), 4783 upregulated genes were related to the term cell part (q = 0.0000), 1647 upregulated genes were associated with the term macromolecular complex (q = 0.0000), 3982 upregulated genes were related to the term organelle (q = 0.0000), and 2441 upregulated genes were related to the term organelle part (q = 0.0000). In the molecular function category, 3228 upregulated genes were associated with the term metallochaperone activity (q = 0.0002) (Additional File 3). In a KEGG analysis, the upregulated genes were mainly involved in the protein processing pathway in the endoplasmic reticulum, proteasome, RNA transport, ribosome biogenesis in eukaryotes, and aminoacyl-tRNA biosynthesis. The upregulated genes were mainly involved in pathways related to cellular processes, environmental information processing, genetic information processing, and metabolism. The species tolerates Cu

ion toxicity by improving growth, division, protein synthesis, and metabolism (matter and energy) (Figure 6a). Only one downregulated gene was involved in each of the Hippo and Hedgehog signaling pathways, styrene degradation, tyrosine metabolism, and oxidative phosphorylation pathways (Figure 6b). Copper is an important trace element that exists in oxidizing and reducing forms and is involved in various biological processes, including redox reactions, enzyme reactions, mitochondrial respiration, iron metabolism, autophagy, and immune regulation. Therefore, maintaining the homeostasis of Cu ions is essential for organisms, as both insufficient and excess Cu can have adverse effects.

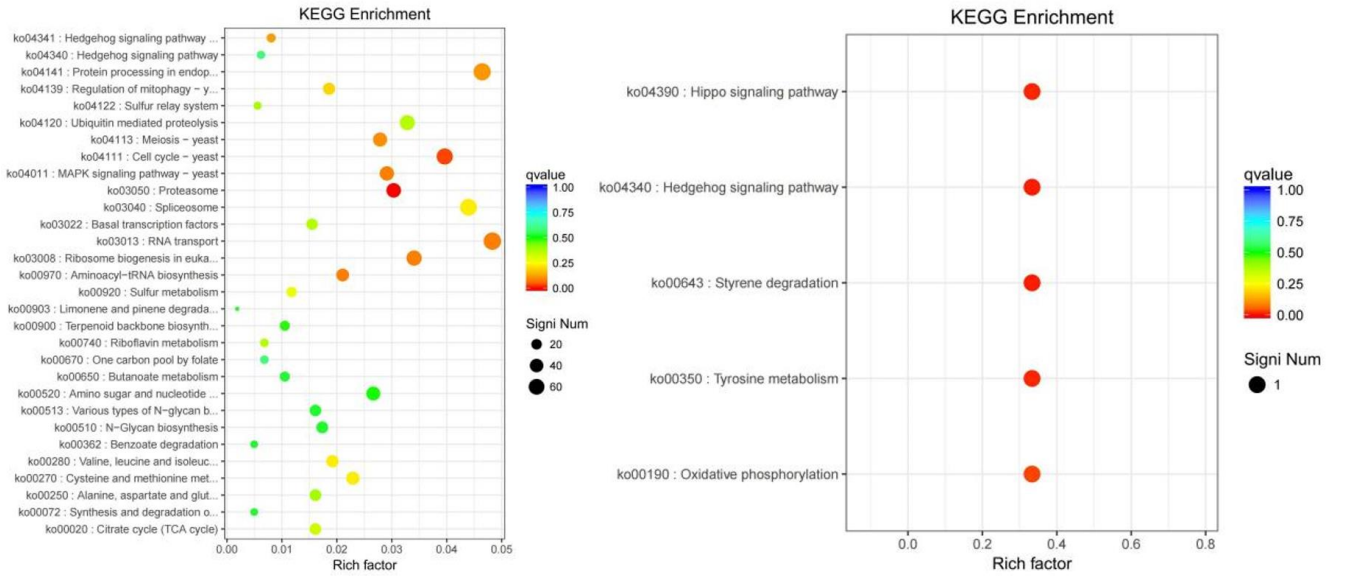

a (up-regulated genes) b (down-regulated genes)

Figure 6*. The enrichment of the differential genes (KEGG database) (B vs C).*

3.3.3. Comparison of Gene Expression Characteristics Between Zn and Cu Stress

Differentially expressed genes between groups A and B were enriched for the terms post-translational modification, protein turnover, chaperones, energy production and conversion, intracellular trafficking, secretion, and vesicular transport according to KOG (Figure 7a). In a GO analysis, differentially expressed genes were mainly enriched for the terms cytoplasmic part, cytoplasm, mitochondrial part, envelope, organelle envelope, mitochondrial membrane, organelle inner membrane, mitochondrion, mitochondrial envelope, and mitochondrial inner membrane. The differentially expressed genes were also involved in mitochondrial structure, protein synthesis, ion transportation, and energy production and conversion.

Downregulated genes in B compared with A ($q < 0.05$) were not enriched for terms in the biological process and cellular component categories. In the molecular function category, 19 downregulated genes ($q = 0.0247$) were enriched for electron carrier activity, and 16 downregulated genes ($q = 0.0582$) were enriched for antioxidant activity (Additional File 4). Upregulated genes ($q < 0.05$) were not enriched for any terms in the three main categories, biological processes, cellular components, or molecular functions, in a GO analysis.

In the biological process category, genes that were down-regulated but did not show significant differences were mainly enriched on the following terms: protein fold, protein transmembrane transport, mitochondrial transmembrane transport, intracellular transmembrane transport and protein transmembrane import into intracellular organelle (Figure 7b). For the cellular component category, the down-regulated genes were mainly enriched for the terms respiratory chain, mitochondrial part, composition and structure of mitochondrion, membrane protein complex, proteasome complex, endopeptidase complex and peptidase complex (Figure 7c). The downregulated genes were enriched for the following terms in the molecular function category: threonin-type endopeptidase activity, threonine-type peptidase activity, oxidoreductase activity, oxidoreductase activity (acting on a sulfur group of donors), and oxidoreductase activity (acting on NADPH) (Figure 7d). In the responses to Zn and Cu stress, genes involved in mitochondria and proteases associated with respiration were inhibited, as was the activity of enzymes involved in protein breakdown and energy production. Additionally, the transport of cell substances was inhibited under Zn stress.

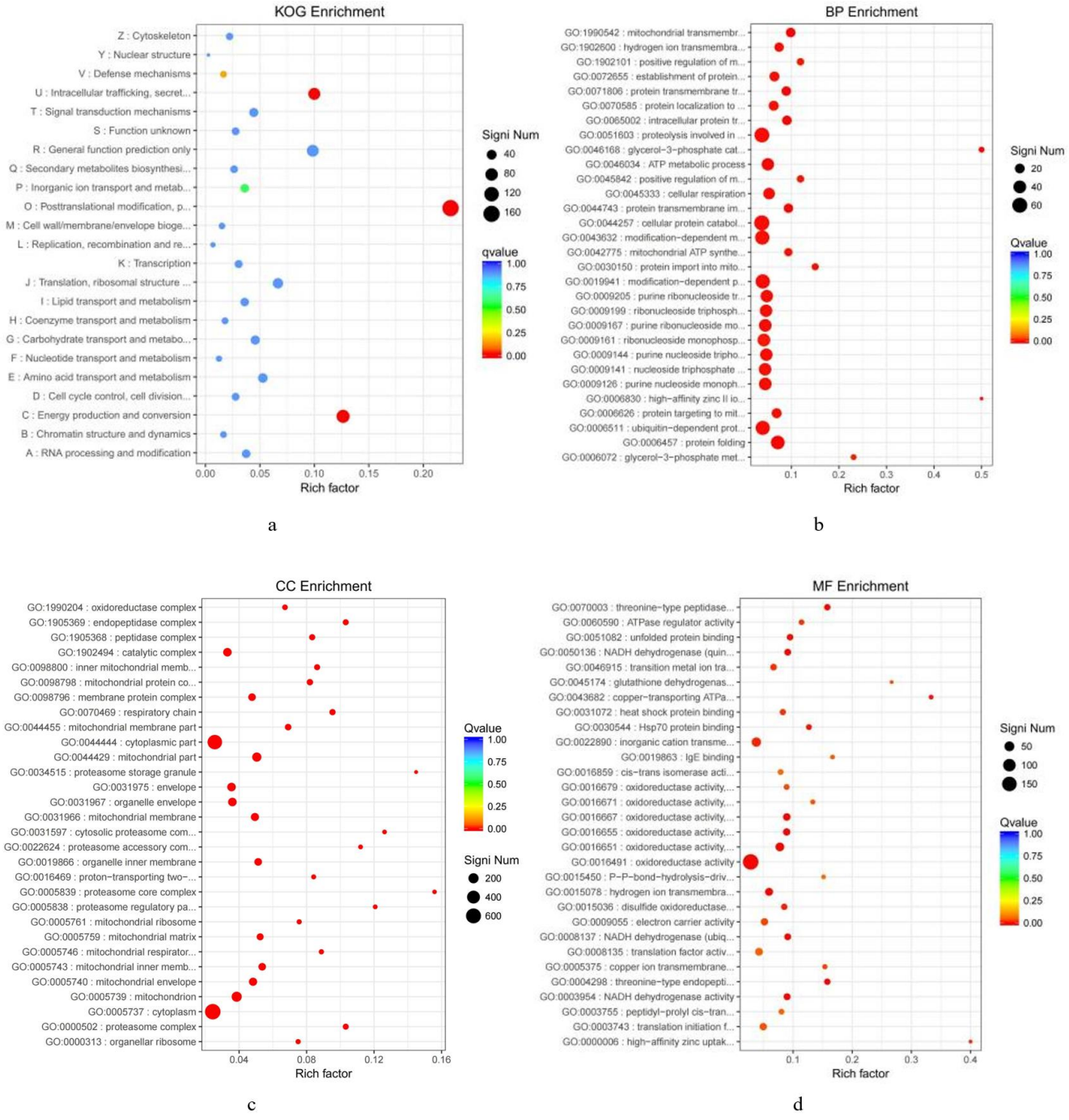

(a- the significantly differential genes in KOG; b,c,d- the down-regulated significantly differential genes in GO)

Figure 7*. The enrichment of the significantly differential genes (A vs B).*

In the KEGG enrichment analysis, upregulated genes were not enriched in any pathway, except carbohydrate metabolism and xenobiotic biodegradation and metabolism under Zn stress. Effects on these two pathways were stronger under Zn stress than under Cu stress (Figure 8a), implying that carbohydrate metabolism improved and exogenous toxic substances were broken down by A. *niger* to a greater extent under Zn stress than under Cu stress. The response of A. *niger* to Cu stress was more positive than that under Zn stress, which may be explained by the role of Cu in many biochemical reactions and the higher toxicity of Cu than Zn. Downregulated genes were not enriched in membrane transport, signaling molecule, or interaction pathways under Zn stress; however, there was enrichment for these terms under Cu stress. There were fewer downregulated genes involved in cell growth and death, cell motility, cellular community, signal transduction, replication and repair, lipid metabolism, xenobiotic biodegradation, and metabolism pathways under Zn stress than under Cu stress; however, there were more downregulated genes involved in

folding sorting and degradation, carbohydrate metabolism, energy metabolism, and overview pathways under Zn stress than under Cu stress (Figure 8b). These results showed that the energy consumption of A. *niger* under Cu stress was greater than that under Zn stress for the bigger toxic effects of Cu [33], and the upregulation of bot h carbohydrate and energy metabolism pathways is not conducive to organic carbon storage in heavy metal-polluted environme nts [34].

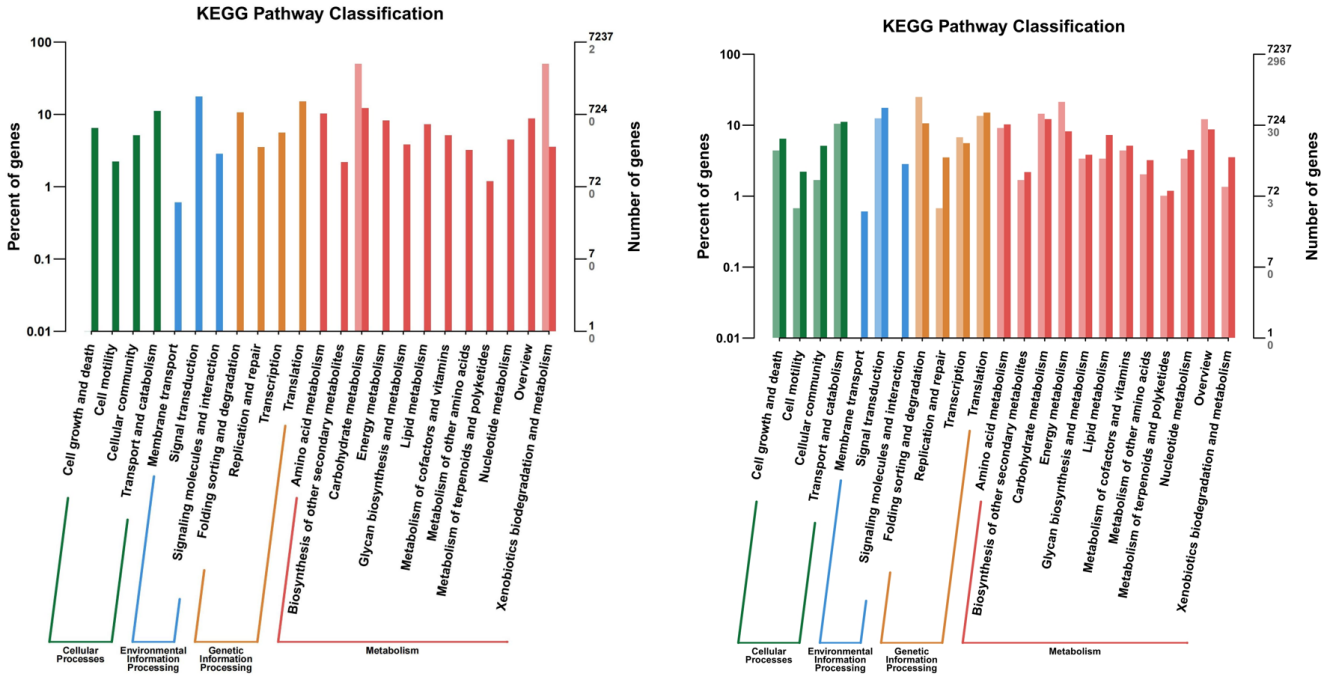

a (up-regulated) b(down-regulated)

Figure 8. *The enrichment of the down-regulated differential genes (KEGG database) (Avs B).*

3.3.4. qRT-PCR Verification

qRT-PCR results are shown in Table 7. The results for 23 genes obtained using qRT-PCR were identical to those of the transcriptomics analysis (82.14%). Only 5 genes showed differences between qRT-PCR and transcriptomics analyses. These differences could be explained by the experimental operation, sample processing, primer designation, data processing and analysis, and selection of genes. For two genes showed inconsistent results, DN33158_c0_g1 (q = 0.0405) and DN35913_c0_g2 (q = 0.0264), the differences between groups may have been insufficient. Genes with larger fold-changes and smaller q-values should be selected for qRT-PCR verification experiments.

This study provides a perspective on the tolerance of Aspergillus niger to heavy metals from the genetic level. Genetic mechanismsun derlying differences in *Aspergillus niger* tolerance to different heavy metals were identified. Although most functional genes were upregulated (and few were downregulated) in response to both Cu and Zn stress, the functions of the upregulated and do wnregulated genes differed, and A. *niger* was more active in response to Cu stress than to Zn stress.

The downregulated genes were associated with organelles with membrane structure and ion transportation, and the up-regulated genes were mainly related to the synthesis of proteins under both Zn and Cu stress.

A. niger tolerates copper and zinc stress in different ways. Under Zn stress, signal transduction and hydrolysis of nuclei c acids were inhibited; cell growth, division, and metabolism of carbohydrates and energy were improved under Cu stress.

Genes involved in the metabolism of carbohydrates and energy production were more highly expressed under Cu stress than under Zn stress, and the consumption of energy was higher under Cu stress than under Zn stress in A. *niger*. The key genes should be confirmed through experiment in future. The study of the microbial commu nity structure, respiration and carbon pool in heavy metal contaminated soil is worthy of in-depth investigation.

Abbreviations

NCBI	The National Center for Biotechnology Information
CASAVA Base Calling	Cluster Analysis and Base Calling Application
CDD	Conserved Domain Database
TrEMBL	Translation of EMBL Nucleotide

	Sequence Database
Swiss-Prot	Swiss Protein Sequence Database
CDS	Coding Sequence
RSeQL	Realizability Semantics Query Language

Acknowledgments

This research was supported by the financial support received from the National Natural Science Foundation of China (52304421), Major Project of Changsha Science and Technology Planning Project (kh2301012), Natural Science Foundation of the Environmental Protection Department of Hunan Province (HBKF2022004), and Research Foundation of the Department of Natural Resources of Hunan Province (Grant No. 20230141ST).

Conflicts of Interest

There is no conflicts of interest.

References

[1] Loa, JDA, Cruz-Rodr ǵuez, IA, Rojas-Avelizapa, NG (2023) Colorimetric detection of metals using CdS-NPs synthesized by an organic extract of *Aspergillus niger*.*Appl. Biochem. Biotechnol.* 195, 4148. https://doi.org/10.1007/s12010-023-04341-z

[2] Nurdin, M Mulkiyan L, Sugiwati S, Abimayu H, Arifin ZS, Muryanto M, Maulidiyah M, Arham Z, Salim LOA, Irwan I (2023) Productivity of *Aspergillus niger* InaCC F57 isolate as cellulase agent in OPEFB hydrolysis for glucose high yield. *BioNanoScience* 13, 114. https://doi.org/10.1007/s12668-023-01066-5

[3] Wu L, Zhang L, Li X, Lv R, Cao W, Gao W, Liu J, Xie Z, Liu H(2023) Effective production of kojic acid in engineered *Aspergillus niger*. *Microb. Cell Factories* 22, 40. https://doi.org/10.1186/s12934-023-02038-w

[4] Amin I, Nazir R, Rather MA (2024) Evaluation of multi-heavy metal tolerance traits of soil-borne fungi for simultaneous removal of hazardous metals. *World J. Microbiol. Biotechnol.* 40, 175. https://doi.org/10.1007/s11274-024-03987-z

[5] El-Mahdy OM, Mohamed HI, Mogazy AM (2021) Biosorption effect of *Aspergillus niger* and *Penicillium chrysosporium* for Cd- and Pb-contaminated soil and their physiological effects on *Vicia faba* L. *Environ. Sci. Pollut. Res. Int.* 28, 67608. https://doi.org/10.1007/s11356-021-15382-4

[6] Xia YT, Guo Q, Qin NN, Tang Y. Tan QJ, Sun HJ, Gao YT, Guo Q, Zhou G(2019) Preparation of *Aspergillus niger* mycelium-chitosan and study on the adsorption performance of Cr(VI.). *Mod. Food Sci. Technol.* 35, 68. https://doi.org/10.13982/j.mfst.1673-9078.2019.2.010

[7] Wei BY, Gao GF, Tian Y, Lu XY, Cao L, Li SX,(2011) Decoloring properties of *Aspergillus niger* to rose bengal and water-soluble color paste. *Acta Sci. CIrcumstantiae* 31, 492. https://doi.org/10.3724/SP.J.1011.2011.00468

[8] Cui H, Liu X, Li K, Cao TT, Cui CW, Wang JY (2019) Mechanism of Hg(II), Cd(II) and Pb(II) ions sorption from aqueous solutions by *Aspergillus niger* spores. *Sep. Sci. Technol.* 55, 848. https://doi.org/10.1080/01496395.2019.1576733

[9] Deng XH, Chen RH, Zhuo SN, Zhou GY, Shi Y(2019) Bioleaching characteristics of heavy metals from polluted soil with indigenous *Aspergillus niger* F2. *J. Biobased Mater. Bioenergy* 13, 401. https://doi.org/10.1166/jbmb.2019.1864

[10] Arshadi M, Esmaeili A, Yaghmaei S(2020) Investigating critical parameters for bioremoval of heavy metals from computer printed circuit boards using the fungus *Aspergillus niger*. Hydrometallurgy 197, 105464. https://doi.org/10.1016/j.hydromet.2020.105464

[11] Bahaloo-HorehN, Mousavi SM, Baniasadi M (2018) Use of adapted metal tolerant *Aspergillus niger* to enhance bioleaching efficiency of valuable metals from spent lithium-ion mobile phone batteries. J. Cleaner Prod. 197, 1546. https://doi.org/10.1016/j.jclepro.2018.06.299

[12] Nguyen TH, Won S, Ha MG, Nguyen DD, Kang HY (2021) Bioleaching for environmental remediation of toxic metals and metalloids: A review on soils, sediments, and mine tailings. Chemosphere 282, 131108. https://doi.org/10.1016/j.chemosphere.2021.131108

[13] Hajihoseini J, Fakharpour M (2019) Effect of temperature on bioleaching of iron impurities from kaolin by *Aspergillus niger* fungal. J. Asian Ceram. Soc. 7, 82. https://doi.org/10.1080/21870764.2019.1571152

[14] Kiskira K, Theopisti L, Ioannis L, Lamprini AT, Charalampos P, Konstantina P, Klaus MO, Fotios T, Elias C, ·Gerasimos L, Maria OP,(2023) Bioleaching of scandium from bauxite residue using fungus *Aspergillus Niger*. Waste Biomass Valorization 14, 3377. https://doi.org/10.1007/s12649-023-02116-5

[15] Deng XH, Chen RH, Shi Y, Zhuo SN (2018) Preliminary bioleaching of heavy metals from contaminated soil applying *Aspergillus niger*. Am. J. Environ. Sci. Eng. 2, 72. https://doi.org/10.11648/j.ajese.20180204.14

[16] Ren WX, Li PJ, Geng Y, Li XJ (2009) Biological leaching of heavy metals from a contaminated soil by *Aspergillus niger*. J. Hazard. Mater. 167, 164. https://doi.org/10.1016/j.jhazmat.2008.12.104

[17] Srichandan H, Mohapatrab RK, Parhib PK, Mishraa S (2019) Bioleaching approach for extraction of metal values from secondary solid wastes: A critical review. Hydrometallurgy 189, 105122. https://doi.org/10.1016/j.hydromet.2019.105122

[18] Tripathi S, Poluri KM (2021) Heavy metal detoxification mechanisms by microalgae: Insights from transcriptomics analysis. Environ. Pollut. 285, 117443. https://doi.org/10.1016/j.envpol.2021.117443

[19] Voigt K, Sharma CM, Mitschke J, Lambrecht SJ, Voß B, Hess WR, Steglich C (2014) Comparative transcriptomics of two environmentally relevant cyanobacteria reveals unexpected transcriptome diversity. ISME J. 8, 2056. https://doi.org/10.1038/ismej.2014.57

[20] Sun S, Wang Y, He B, Chen J, Leng F, Luo W (2024) Comparative transcriptomics revealed the mechanism of Stenotrophomonas rhizophila JC1 response and biosorption to Pb^{2+}. Environ. Geochem. Health 46, 231. https://doi.org/10.1007/s10653-024-02019-x

[21] Wang W, Yan H, Dong G, Li Z, Jiang C, Gu D, Niu D, Zhou D, Luo Y(2022) Comparative transcriptomics reveal different genetic adaptations of biofilm formation in Bacillus subtilis isolate 1JN2 in response to Cd^{2+} treatment. Front. Microbiol. 13, 1002482. https://doi.org/10.3389/fmicb.2022.1002482

[22] Kwon MJ, Jørgensen TR, Nitsche BM, Arentshorst M, Park J, Ram AFJ, Meyer V (2012) The transcriptomic fingerprint of glucoamylase over-expression in *Aspergillus niger*. BMC Genomics 13, 701. https://doi.org/10.1186/1471-2164-13-701

[23] Wang L, Xie Y, Chang J, Wang J, Liu H, Shi M, Zhong Y(2023) A novel sucrose-inducible expression system and its application for production of biomass-degrading enzymes in *Aspergillus niger*. Biotechnol. Biofuels Bioprod. 16, 23. https://doi.org/10.1186/s13068-023-02274-7

[24] Pullan ST, Paul D, Stéphane D, Roger I, Matthew K, Almar N,Jolanda M van M, Raymond W, Martin JB, Sanyasi G, Gregory AT,David BA(2014) RNA-sequencing reveals the complexities of the transcriptional response to lignocellulosic biofuel substrates in *Aspergillus niger*. Fungal Biol. Biotechnol. 1, 3. https://doi.org/10.1186/s40694-014-0003-x

[25] van Munster JM, Jolanda M, van M, Paul D, Stéphane D, Steven TP, Martin JB, Sunir M, Matthew K, Emelie CMN, Kristin W, Richard F, Richard B, Yu XL, Paul D, David BA(2014) The role of carbon starvation in the induction of enzymes that degrade plant- derived carbohydrates in *Aspergillus niger*. Fungal Genet. Biol. 72, 34. https://doi.org/10.1016/j.fgb.2014.04.006

[26] Novodvorska M, Hayer K, Pullan ST, Wilson R, Blythe MJ, Stam H, Stratford M, Archer DB (2013) Transcriptional landscape of *Aspergillus niger* at breaking of conidial dormancy revealed by RNA-sequencing. BMC Genomics 14, 246. https://doi.org/10.1186/1471-2164-14-246

[27] Dubey S, Shri M, Gupta A, Rani V, Chakrabarty D (2018) Toxicity and detoxification of heavy metals during plant growth and metabolism. Environ. Chem. Lett. 16, 1169. https://doi.org/10.1007/s10311-018-0741-8

[28] Benjamini Y, Hochberg Y (1995) Controlling the false discovery rate: a practical and powerful approach to multiple testing. J. R. Stat. Soc. B 57, 289. https://doi.org/10.1111/j.2517-6161.1995.tb02031.x

[29] Livak KJ, Schmittgen TD (2001) Analysis of relative gene expression data using real-time quantitative PCR and the $2^{-\Delta\Delta CT}$ method. Methods 25, 402. https://doi.org/10.1006/meth.2001.1262

[30] Macomber L, Imlay JA (2009) Theiron-sulfur clusters of dehydratases are primary intracellular targets of copper toxicity. Proc Natl Acad SciUSA 106, 8344-9. https://doi.org/10.1073/pnas.0812808106

[31] Liu J, Tan D, Qiu H, Liang Y, Wu H, Yang Y, Zhao H (2025) Unraveling the stress response and biosorption mechanisms of *Aspergillus niger*to rare earth element cerium(III) based on transcriptomics and DNA methylomics. Front. Microbiol. 16, 1674444. https://d oi.org/10.3389/fmicb.2025.1674444

[32] Chatterjee S, Das S (2022) Whole-genome sequencing of biofilm-forming and chromium-resistant mangrove fungus *Aspergillus niger* BSC-1. World J. Microbiol. Biotechnol. 39, 55. https://doi.org/10.1007/s11274-022-03497-w

[33] Shi YX, Tang LY, Shao Q, Jiang YZ, Wang ZJ, Peng C, Gu TT, Li Z(2024) The dynamic roles of intracellular vacuoles in heavy metal detoxification by Rhodotorulamucilaginosa. J Appl Microbiol.135, lxae241. https://doi.org/10.1093/jambio/lxae241

[34] Xu YL, Balaji S, Nanthi B, Binoy S, Yong SO, Zhang W, Cornelia R, Donald S, Mark F, Tony H, Dong ZM (2019) Microbial functional diversity and carbon use feedback in soils as affected by heavy metals. Environ. Int. 125, 478. https://doi.org/10.1016/j.envint.2019.01.071